On the relative importance of stratospheric and tropospheric drivers for the North Atlantic jet response to Sudden Stratospheric Warming events

Hilla Afargan-Gerstman[a] , Bernat Jiménez-Esteve[a] , and Daniela I.V. Domeisen[a b]

[a] *ETH Zurich, Institute for Atmospheric and Climate Science, Zurich, Switzerland*

[b] *University of Lausanne, Lausanne, Switzerland*

Corresponding author: Hilla Gerstman, hilla.gerstman@env.ethz.ch

ABSTRACT: Roughly two thirds of the observed sudden stratospheric warming (SSW) events are followed by an equatorward shift of the tropospheric jet in the North Atlantic, while the other events generally show a poleward shift. It is however not resolved which drivers lead to the large inter-event variability in the surface impact. Using an intermediate complexity atmospheric model, we analyze the contribution of different factors to the downward response: polar cap geopotential height anomalies in the lower stratosphere, downstream influence from the northeastern Pacific, and local tropospheric conditions in the North Atlantic at the time of the initial response. As in reanalysis, an equatorward shift of the North Atlantic jet is found to occur for two thirds of SSWs in the model. We find that around 40% of the variance of the tropospheric jet response after SSW events can be explained by the lower stratosphere geopotential height anomalies, while around 25% can be explained by zonal wind anomalies over the northeastern Pacific region. Local Atlantic conditions at the time of the SSW onset are also found to contribute to the surface response. To isolate the role of the stratosphere from tropospheric variability, we use model experiments where the zonal mean stratospheric winds are nudged towards climatology. When stratospheric variability is suppressed, the Pacific influence is found to be weaker. These findings shed light on the contribution of the stratosphere to the diverse downward impacts of SSW events, and may help to improve the predictability of tropospheric jet variability in the North Atlantic.

1. Introduction

Variability in the strength of the stratospheric polar vortex can have a significant influence on midlatitude weather. In particular, reversals of the westerly winds in the polar stratosphere in mid-winter, known as sudden stratospheric warming (SSW) events (Baldwin et al. 2021), are some of the most spectacular examples of extreme events that can have a downward impact onto the troposphere, linked to changes in the position of the North Atlantic tropospheric jet stream (e.g., Baldwin and Dunkerton 2001; Kidston et al. 2015). SSW events involve a rapid warming of the polar stratosphere by up to 30-40 degrees within a few days (Scherhag 1952), and are typically defined by the reversal of zonal mean westerly wind direction at 10 hPa and 60°N (Charlton and Polvani 2007; Butler et al. 2015, 2017).

Following SSW events, temperature and wind anomalies over the polar cap often propagate downward within the stratosphere, and can give rise to negative phases of the Arctic Oscillation (AO) (Baldwin and Dunkerton 2001) and the North Atlantic Oscillation (NAO) (Scaife et al. 2005; Charlton-Perez et al. 2018; Domeisen 2019), as well as cold air outbreaks over Northern Eurasia and the eastern United States (Kolstad et al. 2010; Lehtonen and Karpechko 2016; King et al. 2019; Lu et al. 2021) and marine cold air outbreaks over the Barents and Norwegian Seas (Afargan-Gerstman et al. 2020).

Such a subsequent tropospheric impact can lead to weather extremes (Domeisen and Butler 2020) with high social and economic impacts, especially when occurring in the highly-populated midlatitude regions, e.g., the "Beast from the East" in 2018 (Karpechko et al. 2018; Rao et al. 2018), and the cold temperature extremes in Greece, northwestern Europe and Texas in January and February 2021 (Wright et al. 2021; Lu et al. 2021). This surface influence can persist for up to two months (Baldwin and Dunkerton 2001), thus providing a potential source of predictability for climate and weather forecasts on subseasonal (Domeisen et al. 2020b) to seasonal time scales (e.g., Scaife et al. 2016; Domeisen et al. 2015; Sigmond et al. 2013).

However, one of the challenges for accurate long-term predictions is the variability of the downward impact after SSW events, as not all SSWs are followed by the same downward response. Around two thirds of SSW events in reanalysis are followed by a downward impact in the North Atlantic (e.g., Karpechko et al. 2017; Runde et al. 2016; Jucker 2016), This impact, also referred to as the "canonical downward response", is characterized by an equatorward shift of the tropospheric

jet and storm tracks over the North Atlantic (Karpechko et al. 2017; Domeisen 2019; Afargan-Gerstman and Domeisen 2020). The remaining one third of SSW events are either followed by a poleward tropospheric jet shift, or weak overall anomalies in the North Atlantic region. Is not well understood which factors determine if an SSW event will be followed by a downward impact, and what is the relative importance of these respective factors. Hence, the existence and strength of the downward influence and, in turn, its importance for the evolution of the tropospheric jet remain difficult to predict. The high variability between the surface impacts of different SSW events raises the question about the factors controlling the variability of the downward coupling.

The variability and existence of a downward coupling following SSW events has been linked with both stratospheric and tropospheric drivers. Potential candidates in the stratosphere include the geometry of the SSW event (i.e., vortex splitting or vortex displacement) (Mitchell et al. 2013; Seviour et al. 2013, 2016), the persistence of lower stratospheric circulation anomalies (Black and McDaniel 2004; Hitchcock et al. 2013a; Maycock and Hitchcock 2015) and their strength (e.g., Karpechko et al. 2017; Runde et al. 2016; White et al. 2020; Rao et al. 2020), the strength of the upward wave activity that precedes the SSW (White et al. 2019), and absorption or reflection of planetary waves in the stratosphere following SSWs (Kodera et al. 2016).

However, the stratosphere is not the sole factor determining the tropospheric impact of SSW events. One such factor is the tropospheric jet state (e.g., Chan and Plumb 2009; Garfinkel et al. 2013; Charlton-Perez et al. 2018; Domeisen et al. 2020a). It has been found that the position of the tropospheric jet in model experiments affects the downward response to stratospheric perturbations (Garfinkel et al. 2013). In addition, the local tropospheric circulation around the time of occurrence of the SSW has been found to play a role for stratosphere–troposphere coupling in the Euro-Atlantic region. For example, the presence of a European Blocking (i.e., a blocking over western Europe and the North Sea) around the onset of SSW events favours a subsequent Greenland blocking (consistent with a negative NAO) as a response to the SSW (Domeisen et al. 2020a), whereas SSWs that occur during cyclonic weather regimes exhibit a weaker response, with a reduced likelihood for an equatorward shift of the North Atlantic jet.

Another factor that may affect the downward influence of the stratosphere is an upstream influence from the Pacific (e.g., Jiménez-Esteve and Domeisen 2018; Afargan-Gerstman and Domeisen 2020). Anomalous circulation patterns in the North Pacific are clearly linked to the phase of the

NAO in the North Atlantic, even without considering a stratospheric influence: The presence of an anomalous ridge (trough) in the Northeast Pacific is associated with a positive (negative) phase of the NAO due to changes in the transient wave propagation and wave breaking over the North Atlantic (Benedict et al. 2004; Franzke et al. 2004; Rivière et al. 2015; Drouard et al. 2015; Jiménez-Esteve and Domeisen 2018). In reanalysis, SSW events that are followed by an equatorward jet shift over the North Atlantic are characterized by an anomalous trough of geopotential height at 500 hPa in the northeastern Pacific and along the western coast of North America, whereas a poleward Atlantic jet shift is often associated with the opposite anomaly in the northeastern Pacific (Afargan-Gerstman and Domeisen 2020). Yet, the relative importance of this link in determining the downward response after SSW events remains unclear.

In the troposphere, the response to SSW events is strongly linked to synoptic eddy feedbacks, which play a role in amplifying the tropospheric response and are responsible for the persistence of the tropospheric jet shift (e.g., Song and Robinson 2004). The absence of synoptic wave feedbacks in the troposphere is shown to result in a poleward shift of the tropospheric jet in response to an SSW (Domeisen et al. 2013). Planetary wave feedbacks also play an important role in forcing the tropospheric circulation in response to stratospheric anomalies (Song and Robinson 2004; Hitchcock and Simpson 2016; Domeisen et al. 2013; Martineau and Son 2013; Smith and Scott 2016). In particular, an analysis of the momentum budget during SSW events implies that the influence of the stratosphere on tropospheric planetary-scale eddies is one of the key mechanisms affecting the tropospheric jet after SSW events (Hitchcock and Simpson 2016). However, this mechanism remains under debate in the literature.

The aim of this paper is to improve our understanding of the downward impact of SSW events in the troposphere by examining the influence of SSW events on tropospheric jet anomalies in an intermediate complexity General Circulation Model (GCM) (Isca, Vallis et al. 2018) and ERA-Interim reanalysis. Our main focus is the relative importance of the three main potential driving factors on the downward influence in the North Atlantic: the strength of the circulation in lower stratosphere, the downstream influence of the northeastern Pacific, and the local conditions in the North Atlantic at the onset of SSW events. Using an intermediate complexity GCM allows for a larger number of SSW events to be analyzed, thus we are not limited by the small sample size of available SSW events in the observational record.

To further quantify the contribution of anomalies in the Pacific circulation and local Atlantic conditions in the absence of stratospheric forcing, we restrict stratospheric variability in a nudged-stratosphere approach.

Details of the model and the nudging experiments, as well as the criterion used for identifying the downward impact, are described in section 2. The influence of potential driving factors is explored in section 3, in the model and reanalysis. Nudged-stratosphere model simulation is analyzed in section 3c. Finally, the main conclusions and a discussion are given in section 4.

2. Methods

a. Intermediate complexity GCM

We use the Isca modelling framework (Vallis et al. 2018), which is based on the Geophysical Fluid Dynamics Laboratory (GFDL) dynamical core coupled with a simplified physics parameterization, including moist and radiative processes. Isca has been previously used to simulate both tropospheric and stratospheric processes. We use the same model configuration as in Jiménez-Esteve and Domeisen (2019). The model uses a Gaussian grid with a horizontal resolution of T42 and 50 vertical levels up to 0.02 hPa, of which 25 lie above 200 hPa. In order to simulate a realistic circulation, we use the multi-band radiation scheme (RRTM) (Mlawer et al. 1997), which allows configurable levels of ozone and CO_2 concentrations (Jucker and Gerber 2017). We use realistic topography and the continental outline from the ERA-Interim reanalysis (Dee et al. 2011). The land-sea contrast is obtained by changing surface characteristics such as mixed layer depth, evaporative resistance and albedo (e.g., Thomson and Vallis 2018).

We perform two types of model simulations: a climatological run with a free stratosphere (used as a control simulation, herein referred to as the FREE run), and a nudged model simulation (herein referred to as the NUDGED run) as in Jiménez Esteve and Domeisen (2020). In the nudged simulation, the zonal mean zonal winds in the stratosphere are relaxed towards the zonal mean seasonal cycle of the control simulation as in Jiménez Esteve and Domeisen (2020). The nudging is confined to pressure levels above the tropopause to avoid nudging winds within the upper troposphere, with a transition layer in the lower stratosphere. This configuration enables us to isolate the tropospheric variability that is independent of stratospheric influence, and to separate the respective influence of the stratosphere and the troposphere on the North Atlantic. The

model uses prescribed fixed sea surface temperatures (SST) following the 1958–2016 monthly SST climatology from NOAA ERSSTv4 (Huang et al. 2015) (daily values are linearly interpolated). For the free stratosphere run, the model is run for 20 years (spin-up) until reaching an equilibrium state, and then run freely for 130 years. The nudged stratosphere simulation is initialized from the same initial conditions (after spin-up) and integrated for 80 years. In sections where both nudged and free stratosphere runs are used, the first 80 model years (after spin-up) from each simulation are analyzed.

b. Detection of SSW events

We define SSW events following the criteria described in Charlton and Polvani (2007). For each SSW event, the central date is defined when the daily-mean zonal wind at 10 hPa and 60°N becomes easterly for the first time between November and March. To ensure a separation into distinct events, two consecutive SSW events are considered to be separate events if a period of 20 days passes between the time the winds return to westerly and the subsequent event (Butler et al. 2017). In total, 91 SSW events are identified between November and March (NDJFM) in the control run.

For comparison with reanalysis, we use the ERA-Interim reanalysis (Dee et al. 2011) for the period 1979–2019. SSW events for the period 1979–2014 are detected according to Butler et al. (2017) for ERA-Interim. Two additional SSW events beyond the period included in Butler et al. (2017) occurred on the 12th of February 2018 and 2nd of January 2019 and are included in this study. Between 1979 and 2019, 26 SSW events are identified (e.g., see updated list in Afargan-Gerstman and Domeisen 2020, Table 1).

c. Downward impact of SSW events

We focus on the North Atlantic, where the downward impact of the stratospheric signal to the troposphere after SSW events is most pronounced (e.g., Butler et al. 2017). To identify the downward impact in the model, we use the same criterion as in Afargan-Gerstman and Domeisen (2020), which is based on the zonal wind anomaly at 300-hPa averaged over the midlatitude North Atlantic (ATL U'300, shown by the black box in Fig. 1). We classify a "canonical downward response" for SSWs as an average negative zonal wind anomaly over the midlatitude Atlantic over

a period of 30 days after the SSW central date, which corresponds to an equatorward shift of the North Atlantic jet. In contrast, SSW events followed by mean positive zonal wind anomalies in this region are defined as having a non-canonical downward response and correspond to a poleward Atlantic jet shift. A qualitatively similar detection of surface impacts can be obtained using a criterion based on the NAO index (Domeisen 2019; Hall et al. 2020), or by other classifications of SSW events with a downward impact (e.g., Karpechko et al. 2017; Runde et al. 2016; Jucker 2016). Most of these classifications are based on the Northern Annular Mode (NAM) index or mixing stratospheric and tropospheric indicators, while the criterion defined here is limited to the troposphere and focused particularly on the North Atlantic region, where the downward influence on the tropospheric circulation is strongest.

d. Contributing factors

In this study, we compute three indices based on the dominant contributing factors to assess the tropospheric response following SSW events:

- Tropospheric zonal wind anomaly in the North Atlantic (ATL U'300): zonal wind averaged between 300–340°E and 45°–60°N, shown by the black box in Fig. 1c).

- Lower-stratosphere geopotential height (NH Z'100): geopotential height anomaly averaged over the polar cap (60°–90°N) at the 100 hPa level.

- Tropospheric zonal wind anomaly in the northeastern Pacific - North America sector (PCF U'300): zonal wind averaged between 220–260°E and 45°–60°N, shown by the red box in Fig. 1d).

All anomalies (indicated by the primes in index names) are computed with respect to the daily climatology, calculated for the period 1979–2019 in ERA-Interim reanalysis, and for 131 years of model integrations in the Isca model. Area weighting is done when computing averages across latitude bands.

3. Results

a. The downward impact of SSW events in reanalysis and in the model

In Fig. 1, a comparison of 300-hPa zonal winds between ERA-Interim and Isca is shown. Overall, the climatological zonal wind speed (shown by the black contours) in the North Atlantic is found to be stronger in the model than in reanalysis. SSW events are followed by a negative zonal wind anomaly over the midlatitude Atlantic, both in reanalysis and in the model, (Fig. 1a,d), thus providing an indicator for the downward tropospheric response in this region.

In the model, negative zonal wind anomalies after SSW events are found following roughly two thirds of SSWs (62 out of 91, equivalent to ~68%) (Fig. 1e), and a mean positive response is found for the remaining one third of SSW events (29 out of 91, equivalent to ~32%) (Fig. 1f). These anomalies correspond to equatorward and poleward shifts of the North Atlantic jet. This ratio between negative and positive zonal wind anomalies is very similar to the ratio found in reanalysis, where 69% of SSWs have a negative zonal wind anomaly in the North Atlantic (Afargan-Gerstman and Domeisen 2020) (Fig. 1b,c). A similar ratio is found by Karpechko et al. (2017) in both ERA-Interim and NCEP/NCAR reanalysis using the NAM index as a criterion to define whether the SSW signal reaches the troposphere. Here, we analyze the Atlantic response for a period of 30-days after SSWs, but consistent results are obtained using a longer period (see Supplementary Fig. S2).

One notable difference between reanalysis and the model is that the zonal wind anomalies in the northeastern Pacific and along the northwestern coast of North America are weaker in reanalysis compared to the model response. Particularly, positive wind anomalies in these regions are stronger for SSW events with a poleward Atlantic jet (Fig. 1f) - a response which is not present in the reanalysis (Fig. 1c). Interestingly, anomalous circulation patterns in the northeastern Pacific have been previously linked to a non-canonical downward impact of SSWs in the North Atlantic (Afargan-Gerstman and Domeisen 2020). We further investigate this relation in the next sections.

The similar ratio between the model and reanalysis with respect to equatorward versus poleward zonal wind responses to SSW events in the North Atlantic suggests that the model provides a good testing ground for the variability of the downward impact. A further analysis of how SSW events affect the Atlantic jet response is obtained using jet latitude detection in ERA-Interim reanalysis.

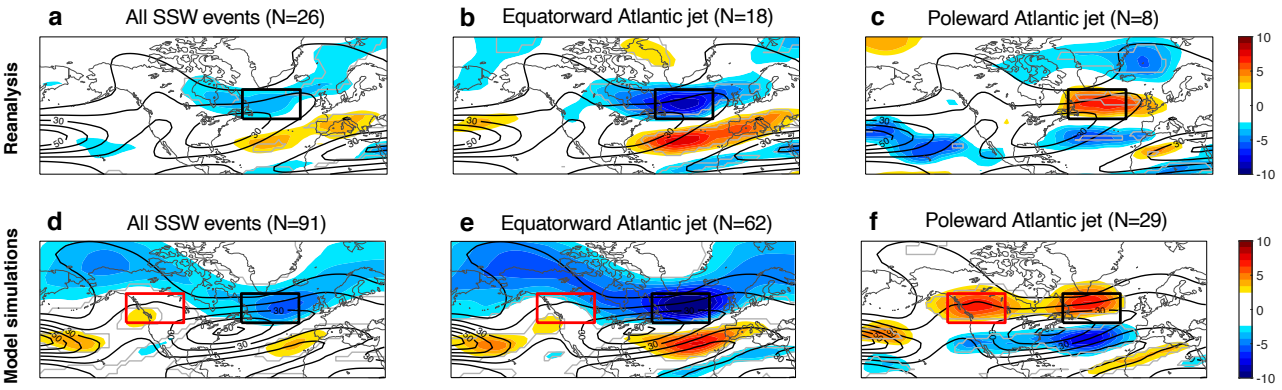

220 FIG. 1. (a-c) Zonal wind anomalies (color shading, m s^{-1}) after (a) all SSW events, (b) SSW events followed
221 by a negative zonal wind anomaly, and (c) SSW events followed by a positive zonal wind anomaly in the North
222 Atlantic (45°N to 60°N, 300°E to 340°E, indicated by the black box) in ERA-Interim reanalysis (1979–2019).
223 Anomalies are averaged over a period of 30 days after the central date of the SSW events. Black contours show
224 the DJF climatology of the zonal wind field (10 m s^{-1} intervals starting from 10 m s^{-1}). (d-f) Same as (a-c) but
225 for the model. Regions within grey contours in all panels correspond to anomalies that are significant at the 95%
226 confidence level (calculated using a Student's t-test).

231 We compare between jet latitude in November to March (NDJFM) climatology (dashed curve,
232 Fig. S1a) and 1-30 days after SSWs (solid curve). Following SSW events, there is a higher
233 probability of a central and southern jet latitude, compared with the three preferred jet positions
234 described in Woollings et al. (2010): "northern", "central" and "southern" jet latitudes. Similar to
235 reanalysis, SSW events in the model are followed on average by an equatorward shift of the eddy-
236 driven jet compared to the model NDJFM climatology (solid and dashed black curves, respectively,
237 in Supplementary Fig. S1b). SSWs with a negative 300-hPa zonal wind anomaly (in blue, Fig. S1a)
238 are followed by an equatorward shifted jet distribution of around 6° latitude compared to SSWs
239 with positive zonal wind anomalies (in red), as expected by the Atlantic U'300 definition. A
240 similar response is found in the model (Fig. S1b). This analysis thus confirms the usefulness of the
241 classification method used in this paper and further confirms that the model is a useful tool for our
242 analysis.

b. Tropospheric circulation response to SSWs associated with the selected drivers

As a next step, we investigate what determines the sign of the response to SSW events. Three potential remote drivers are here suggested to influence the sign of the North Atlantic tropospheric jet response to SSWs: the strength of lower stratospheric anomalies, the tropospheric circulation in the Pacific, and local conditions in the North Atlantic.

Lower stratospheric anomalies are considered one of the essential ingredients for the downward impact. The persistence of tropospheric anomalies after SSW events is found to be strongly dependent on whether the stratospheric anomalies induced by the SSW event reach the lower stratosphere (Hitchcock et al. 2013b). A slow recovery of lower stratospheric anomalies after SSW events, which can persist up to 2 months, has been shown to be linked to SSWs with a stronger canonical downward impact. In agreement, smaller magnitude and shorter persistence of the lower stratospheric anomaly after SSW events contributes to a lack of a tropospheric impact for SSWs (Karpechko et al. 2017).

To examine the dependence of the downward impact of SSW events (measured by the tropospheric jet anomaly in the North Atlantic) on these drivers, we define an index for each driver (see section 2d) and investigate the relation between these indices and the downward response in the North Atlantic region.

For the lower stratospheric influence, we use the polar cap geopotential height anomaly at 100 hPa (NH Z'100 hereafter) as a measure of the circulation response in the lower stratosphere, which has been shown to be strongly correlated with the NAM index (e.g., Baldwin and Thompson 2009; Runde et al. 2016). For the northeastern Pacific influence, the zonal wind anomaly averaged over the northeastern Pacific and over the western coast of North America is used as an index (PCF U'300). Both the NH Z'100 and the PCF U'300 indices are averaged between days 1 and 30 after the SSW events. The local Atlantic conditions are defined using the same index as the downward impact (ATL U'300), but for the period between -2 and 2 days with respect to the SSW onset dates.

Using the criterion based on the lower stratospheric index (NH Z'100), the influence of the lower stratosphere on the downward impact is demonstrated (Fig. 2a-d). We can distinguish between two types of responses: most SSW events exhibit a positive NH Z'100 index after SSW events, both in the model (78 out of 91 SSWs) and the reanalysis (22 out 26 SSWs) (Fig. 2a,c). For the SSWs that were followed by a negative NH Z'100 response, no clear downward impact is found in the North

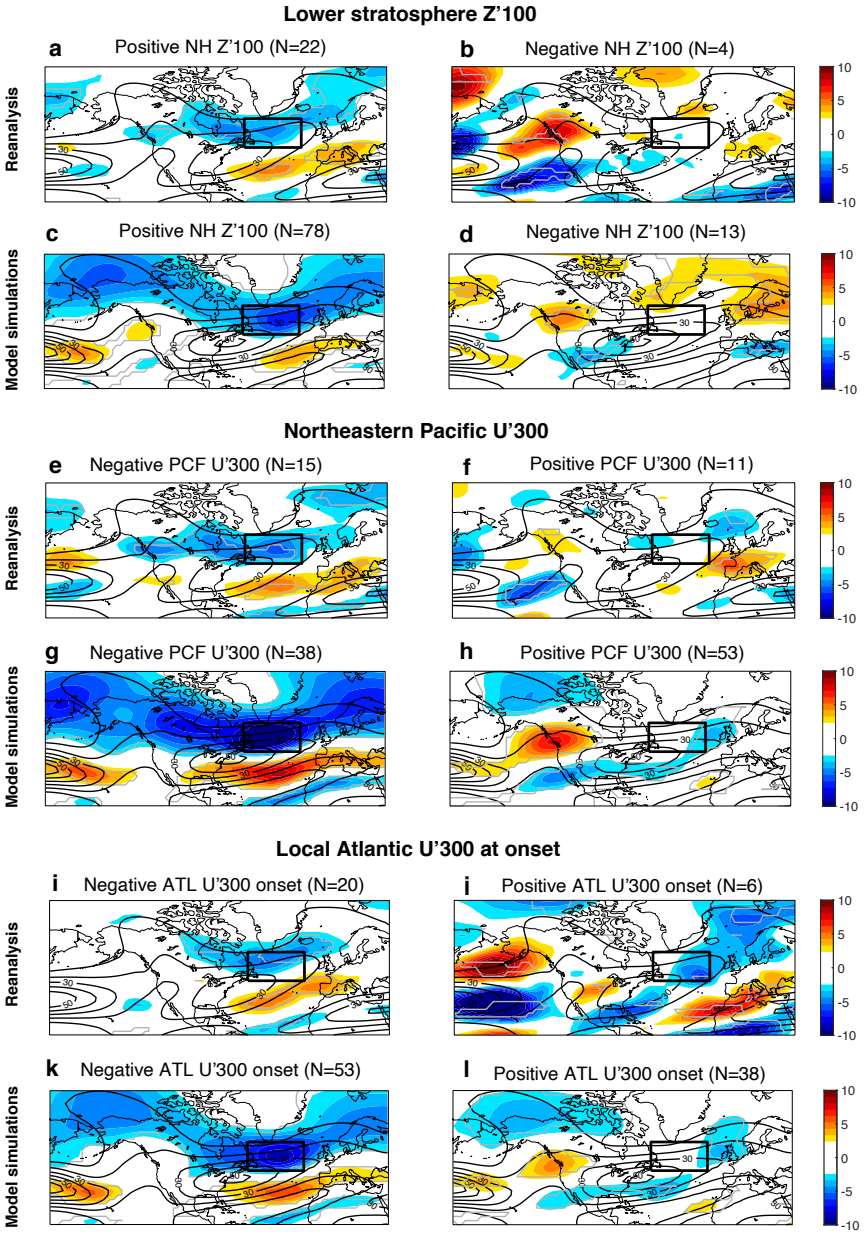

FIG. 2. Same as Fig. 1, but for criteria based on the lower stratosphere (NH Z'100 index, averaged between 1 to 30 days), the northeastern Pacific (U'300, between 1 to 30 days), and the Atlantic (U'300, between days -2 and 2) in ERA-Interim and model simulations. All periods are with respect to SSW central date. (a-d) SSW events followed by (a,c) a positive polar cap NH Z'100 index, and (b,d) a negative NH Z'100 index in (upper panels) the reanalysis and (lower) the model. (e-h) Same as (a-d), but for criterion based on anomalous circulation in the northeastern Pacific after SSWs, and (i-l) criterion based on local Atlantic conditions at the time of SSW onset. Black contours indicate the DJF climatology of the zonal wind field (10 m s^{-1} intervals starting from 10 m s^{-1}). Grey contours in all panels indicate anomalies at the 95% significance level (calculated using a Student's t-test).

Atlantic in terms of tropospheric zonal wind anomalies (Fig. 2b,d), although there is a westerly wind anomaly extending over northern Europe in the model. One of the dominant features in the negative NH Z'100 response is the presence of positive zonal wind anomalies over the northeastern Pacific and the western coast of North America (Fig. 2b,d). These anomalies are significant both in the reanalysis and in the model, suggesting a link to the contribution of the Pacific driver for these events.

The link between the northeastern Pacific wind anomalies and the Atlantic circulation during SSW events can also be demonstrated by using the PCF U'300 index as a criterion. This yields two composites: SSWs that are followed by a negative Pacific index (15 out of 26 SSWs in reanalysis and 38 out of 91 in the model), in which the general tropospheric response is characterized by negative zonal wind anomalies over the midlatitudes (Fig. 2e,g), and in contrast events that are followed by a positive Pacific index (11 out 26 SSWs in reanalysis and 53 out of 91 in the model), in which there is no downward impact in the North Atlantic (Fig. 2f,h). Despite the different frequency of SSWs with a negative or positive Pacific index, the sign of the Atlantic response in these composite is consistent between the reanalysis and the model.

A negative (positive) North Atlantic precursor is defined when the ATL U'300 index is negative (positive) averaged over days -2 to 2 with respect to the central date of a SSW event (i.e., SSW onset). Using this criterion yields two composites which represent the local Atlantic conditions at the time of SSW onset. The majority of SSWs are found to be associated with a negative Atlantic index at the onset (20 out of 26 SSWs in reanalysis and 53 out of 91 in the model). These SSWs are followed by a negative response in the midlatitude Atlantic after SSW events (Fig. 2i,k). SSWs with a positive Atlantic index at the onset are also followed by an average negative zonal wind anomalies both in the reanalysis and in the model, although the response is weaker in the model and slightly shifted eastward (Fig. 2j,l).

1) Correlation analysis between the North Atlantic jet response and dynamical drivers

Next, we investigate the respective relationships between the 30-day average Atlantic jet response after SSW events and the selected drivers shown in the scatter plots in Fig. 3. Following SSW events, the North Atlantic jet anomaly is found to be negatively correlated ($r=-0.63$, $p<0.01$) with the lower stratospheric polar cap geopotential height anomaly (Fig. 3a). This relation explains

about 40% of the variance of zonal wind anomalies in the Atlantic in the aftermath of SSW events in the model, compared to 20% of the variance in the reanalysis, which suggests stronger downward coupling in the model. Consistent with Fig. 2, we find that for the majority of SSWs (84% of SSWs in reanalysis, and 85% of SSWs in the model), positive geopotential height anomalies in the lower stratosphere after SSWs are accompanied by negative zonal wind anomalies over the midlatitude North Atlantic (Fig. 3a). On average, the stratospheric forcing in the model is stronger than in the reanalysis (as represented by the red and green triangles in Fig. 3a for the model and the reanalysis, respectively).

The analysis shown in Fig. 2e-h suggests that negative Atlantic zonal wind anomalies after SSW events are associated with a negative sign of the northeast Pacific index, while a positive Pacific index is associated with a weak, close to zero Atlantic signal. Consistent with that, we find a positive relationship between Atlantic zonal wind anomalies and the northeast Pacific index, with a significant positive correlation ($r=-0.68$, $p<0.01$) in the aftermath of SSW events in the model (Fig. 3b). A negative northeastern Pacific response occurs for nearly 57% of SSWs in reanalysis, while in the model this ratio is lower (around 40%). Also, in the model it is found that 46% of Atlantic jet variability can be explained by the correlation with the northeastern Pacific index. A similar yet weaker relation is found in reanalysis, where the northeastern Pacific jet explains about 26% of the North Atlantic jet response after SSW events. Note that the variability of the Pacific circulation in the model excludes ENSO variability by experimental design (i.e., climatological SST).

In the Atlantic region, local zonal wind anomalies (ATL U'300) around the time of the onset of the SSW event (days -2 to 2) are positively correlated with the anomalies after the event (days 1 to 30) (Fig. 3c), consistent with the composite analysis using the onset conditions as a criterion, shown in Fig. 2i-l. Thus, a negative ATL U'300 index at the onset of SSW events is associated with an equatorward shift of Atlantic wind anomalies, whereas a positive ATL U'300 index at the time of the onset is related to a weak Atlantic response. This relation explains a larger fraction of the variability in the downward response in the model than in reanalysis (the correlation is not statistically significant in reanalysis, suggesting that in the model the tropospheric wind response in the Atlantic is more persistent and has a stronger autocorrelation with the onset conditions.

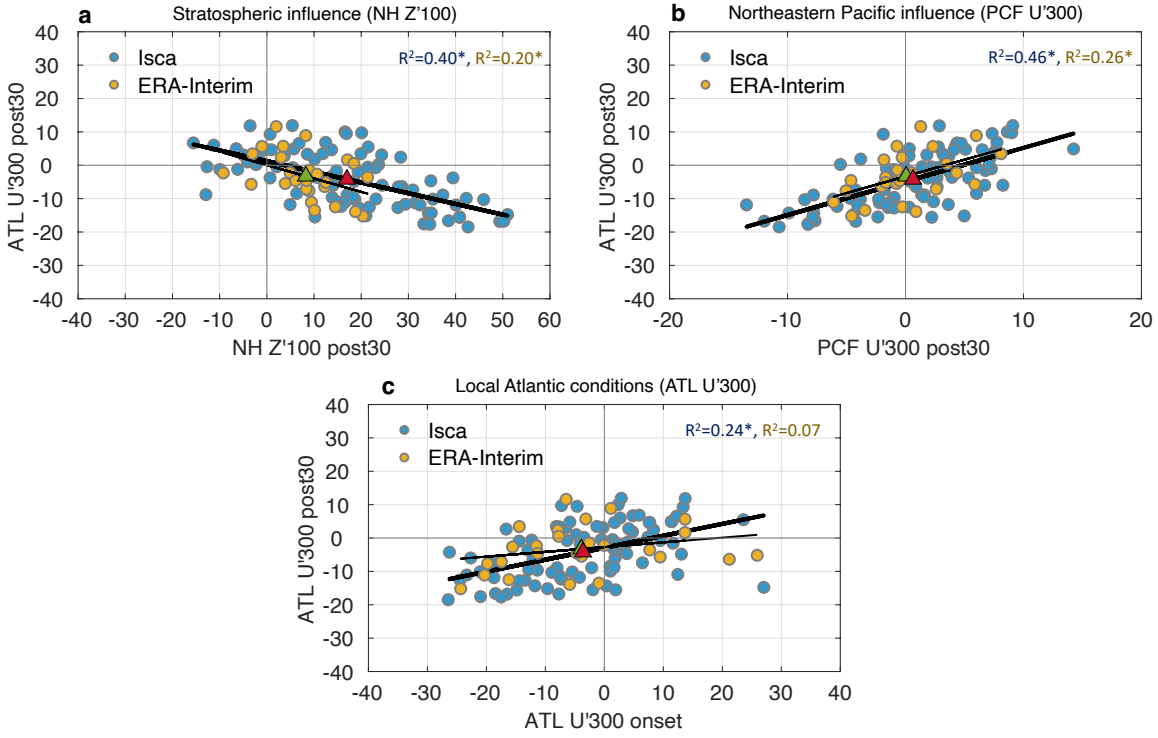

318 FIG. 3. Relationship of the 300-hPa Atlantic zonal wind anomaly with selected indices following SSW events
319 in Isca (blue) and in ERA-Interim reanalysis (yellow). The relationship between (a) the North Atlantic zonal
320 wind anomalies at 300 hPa (ATL U'300) and the Northern Hemisphere polar cap Z'100 index in the aftermath
321 of SSW events (days 1 to 30). (b) The relationship between Atlantic U'300 and the northeastern Pacific zonal
322 wind index (PCF U'300), both in the aftermath of SSW events, and (c) between Atlantic U'300 after SSW events
323 (days 1 to 30) and the Atlantic U'300 at the onset of the event (days -2 to 2). R^2 values are shown in each panel
324 for both model (blue) and reanalysis (yellow). All statistically significant correlations are marked by an asterisk,
325 with p-values < 0.01. The black lines show the linear fit for the model (bold) and reanalysis (thin), respectively.
326 Red and green triangles represent the mean values in the model and in reanalysis, respectively.

348 We repeated the same analysis as in Fig. 3 for different averaging periods (see Table 1 in the
349 Supplementary). The results are qualitatively similar. Compared to a 30-day period, longer
350 averaging periods lead to stronger correlations between the stratospheric and the northeastern
351 Pacific drivers and the North Atlantic zonal wind anomalies in the model. These correlations are
352 found to be weaker in the reanalysis. Interestingly, particularly high correlations are found for local
353 Atlantic conditions in both the model and the reanalysis when a period of 1-10 days after SSW
354 events is considered (right column in Table S1), suggesting that the predictive information arising

from the North Atlantic can be attributed to this initial period. These correlations persist longer in the model compared to reanalysis, which is expected given that idealized models often have decorrelation timescales that are too long compared to reanalysis (Chan and Plumb 2009; Gerber and Polvani 2009). Lower correlation with the onset conditions are found when longer periods are considered.

2) Fraction of Atlantic jet shifts for stratospheric and tropospheric drivers

To investigate the relative importance of the stratospheric versus the tropospheric drivers, we compute the fraction of SSWs with equatorward versus poleward jet shifts in the North Atlantic under various conditions represented by each of the three indices shown in Fig. 3. Figure 4 shows the fraction of SSWs as a function of the time lag between the Atlantic jet shift and the central date of the SSWs. The indices representing stratospheric or tropospheric conditions are evaluated at each lag, except for the local Atlantic driver, which is defined as days -2 to 2 with respect to the onset of the SSW event.

We separate the analysis between equatorward (Fig. 4a,b) and poleward (Fig. 4c,d) Atlantic jet shifts. On average, there are 18 SSW events with an equatorward jet shift in the reanalysis and 62 events in the model, and 8 SSW events with a poleward jet shift in the reanalysis and 29 events in the model. At each time lag, however, the fraction of SSWs with the selected stratospheric or tropospheric conditions is determined out of the total number of SSWs with an equatorward or poleward jet shifts at this lag. For example, at a lag of 5 days the fraction of SSWs with an equatorward jet shift in the Atlantic and positive lower stratospheric circulation anomalies is determined by the number of SSWs that have a negative ATL U'300 and positive Z'100 at this lag. For comparison, the fraction of SSWs with an equatorward Atlantic jet shift at a lag of 5 days and positive local Atlantic conditions is the number of SSWs that have a positive ATL U'300 at this lag and a negative ATL U'300 at the SSW onset. The significance is estimated by a bootstrap re-sampling method using 1000 random selections with replacement from the original sample.

A positive geopotential height anomaly in the lower stratosphere (dark blue bars in Fig. 4) is the most prominent condition for an equatorward jet shift response after the onset of SSW events, occurring in more than 80% of SSWs with equatorward jet shift response in the model (Fig. 4b) and in the reanalysis (Fig. 4a). Similarly, negative zonal wind anomalies in the Atlantic region

at the onset of SSW events (dark yellow bars in Fig. 4) characterize a large fraction of the SSWs with an equatorward jet shift response also beyond the onset time. This high fraction persists also at longer lags, consistent with the enhanced persistence of lower stratospheric anomalies and tropospheric circulation anomalies after SSWs. A larger fraction of SSWs with an equatorward Atlantic jet response is also found for negative Pacific zonal wind anomalies around lag 0 (dark red bars in Fig. 4a,b), while positive Pacific conditions tend to become more frequent at longer lags (light red bars).

A poleward jet response after SSW events is characterized by an interplay between stratospheric and tropospheric drivers, both in the reanalysis and in the model (Fig. 4c,d). The fraction of SSWs with a poleward Atlantic jet response (i.e., positive zonal wind anomalies) is increased after lag 5 for positive Pacific wind anomalies (light red bars) in the model (Fig. 4d), and after lag 10 in the reanalysis (Fig. 4c). This suggests that a poleward Atlantic jet response occurs more frequently at shorter lags in the model compared to reanalysis. A consistent behaviour is found under positive lower stratospheric geopotential height anomalies (dark blue bars). Overall, nearly 80% of SSWs with a poleward Atlantic jet response in the model are associated with positive Pacific conditions (light red bars in Fig. 4d). Equatorward wind anomalies in the Atlantic at the time of the SSW onset (around lag 0) are found to be associated with a higher fraction of SSWs with a poleward jet response at longer lags, particularly in reanalysis (dark yellow bars in Fig. 4c).

Overall, we find that strongly positive geopotential height anomalies in the lower stratosphere and negative zonal wind anomalies in the Northeast Pacific are both linked with a canonical Atlantic response (i.e., negative ATL U'300, Fig. 3a,b) during days 1 to 30 after SSWs. In contrast, weak positive or negative geopotential height anomalies in the lower stratosphere during this period are associated with a weaker canonical Atlantic response or a poleward Atlantic jet shift (i.e., positive ATL U'300, Fig. 3a). This relationship is similar both in the model and in reanalysis, yet with a lower correlation in reanalysis. A poleward Atlantic jet shift is also found to be associated with more positive northeastern Pacific anomalies, in the model as well as in the reanalysis (Fig. 3b).

For comparison, the correlation of the Atlantic jet response with local Atlantic conditions at the time of the SSW event onset is found to be weaker relative to the lower stratospheric and Pacific indices, both in the model and in the reanalysis (Fig. 3c), particularly for periods longer than 10 days (see Table 1 in Supplementary). Yet, despite the relatively weak correlation, for the majority

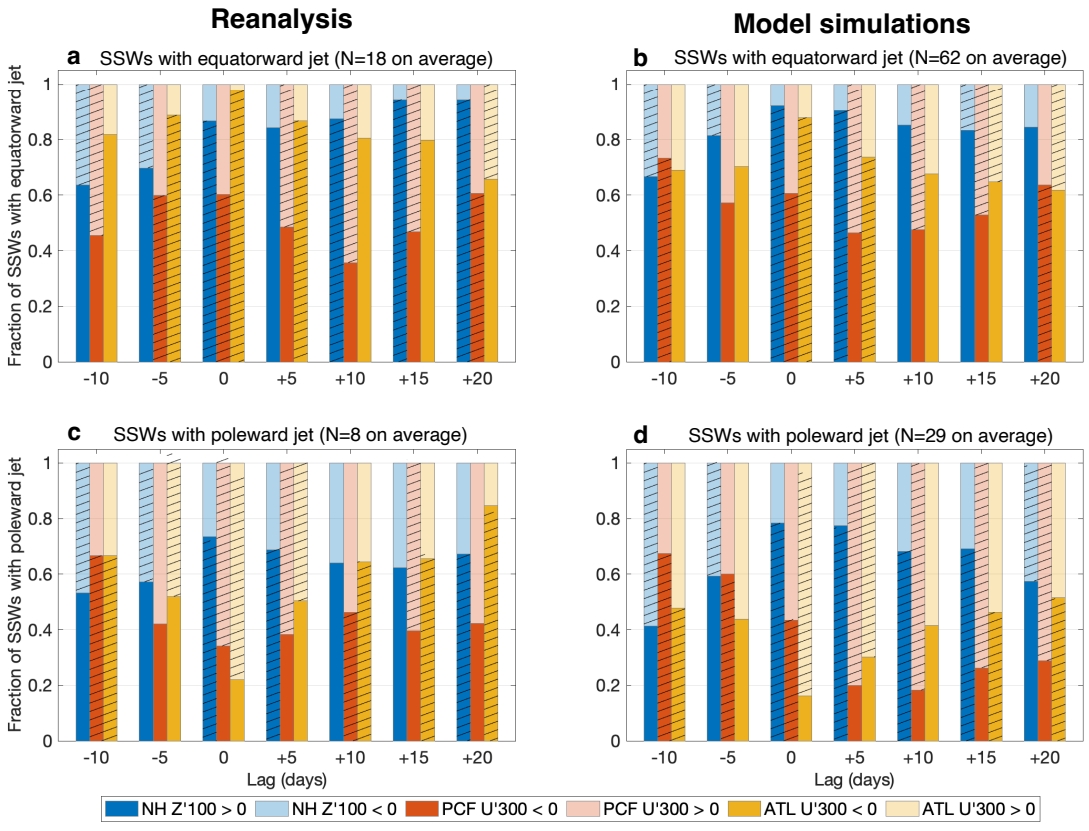

402 FIG. 4. Fraction of SSWs with an (upper panels) equatorward and (lower) poleward jet shifts in the North
403 Atlantic under selected stratospheric and tropospheric conditions as a function of time lag, with respect to the
404 SSW central date, in (a,c) reanalysis and (b,d) model simulations. An equatorward or a poleward response is
405 based on the 300-hPa Atlantic zonal wind index (ATL U'300) at each lag. Lower stratospheric (NH Z'100) and
406 Pacific (PCF U'300) indices are evaluated for each lag, whereas for the local Atlantic conditions we use Atlantic
407 zonal wind index (ATL U'300) in days -2 to 2 with respect to the SSW event onset. Smoothing is performed
408 using a running mean with a 5-day window, and plotted at 5-day intervals. Values statistically significant at the
409 90% level are indicated by a hatching. Note that the fraction of SSWs on the y-axes shows the number of SSWs
410 with the selected conditions out the total number of SSWs with equatorward or poleward shifts.

423 of SSW events an equatorward shift of the North Atlantic jet tends to be consistent with the initial
424 tropospheric response in this region (Fig. 2i,k), as also demonstrated by the persistence of local
425 Atlantic conditions over timescales longer than 10 days (Fig. 4a,b). These correlations persist
426 longer in the model compared to reanalysis.

We note that the correlation with the lower stratosphere and northeastern Pacific indices does not provide predictive information for the downward impact of SSW events, as the indices are defined over the same period as the downward response.

c. The role of the troposphere in the absence of stratospheric forcing

In this part of the paper, we evaluate the contribution of the stratosphere to the frequency of equatorward versus poleward jet shifts over the midlatitude Atlantic. To do so, we compare the results of the free-stratosphere run (i.e., with a freely evolving stratosphere, and hence, with SSW events) to a model simulation with a stratosphere nudged to climatology, which does not exhibit extreme events such as SSWs. This approach artificially removes the lower stratospheric influence in the model, thus allowing us to isolate the role of the northeastern Pacific remote influence on the Atlantic jet position, as well as the role of local Atlantic conditions from the stratospheric forcing.

As shown in the previous sections, the most prominent surface response after SSW events in observations is an anomalous equatorward shift of the North Atlantic jet (Fig. S1a). In addition to the equatorward jet response, previous work has shown that SSWs are followed by an increased frequency of the negative NAO phase and a transition from a positive to a negative NAO (Charlton-Perez et al. 2018; Domeisen 2019). A similar behaviour is expected to be found for Atlantic jet shifts in the model. Therefore, we compare the distributions of the frequency of equatorward and poleward jet shifts in model simulations with/without a free stratosphere. This comparison allows us to evaluate to what extent stratospheric variability contributes to a more frequent equatorward jet.

For this purpose, we first evaluate the frequency of Atlantic jet shifts, defined as the number of days out of a 45-day period in which the zonal wind anomaly at 300 hPa and over the Atlantic sector is in a particular phase, i.e. a positive or negative sign of the anomaly. We find that equatorward jet shifts in the model tend to occur for nearly 43 days (out of 45 days) in the FREE run (shown in blue in Fig. 5a) compared to 27 days in the nudged stratosphere run (in purple), in which SSW events cannot occur, denoting a skewness towards a more frequent occurrence in the free stratosphere run. Interestingly, poleward jet shifts occur for larger number of days in the FREE run (in red) compared to the nudged stratosphere run (in orange, Fig. 5b), most often occurring for around 27 days within a 45-day period (Fig. 5b).

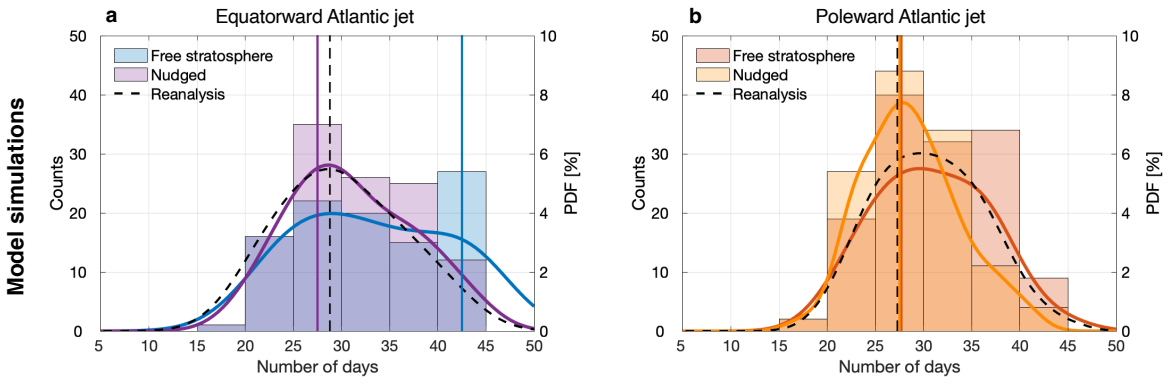

456 FIG. 5. Histograms of the frequency of daily zonal wind anomalies ($m\ s^{-1}$) at 300 hPa in the North Atlantic
457 (black box in Fig. 1c) during NDJFM for (a) equatorward, and (b) poleward jet shifts. The frequency of Atlantic jet
458 shifts, defined as the number of days out of 45 days with equatorward (negative) or poleward (positive) anomalies,
459 is shown in model simulations with a free stratosphere (blue/red) and a nudged stratosphere (purple/orange). Only
460 frequencies greater than 15 days are shown. For each composite, we plot the kernel density estimation for the
461 equatorward and poleward zonal wind anomalies (solid curve). All probability density functions are normalized
462 for comparison. Equatorward and poleward jet shift events in ERA-Interim reanalysis during NDJFM (between
463 1979 to 2019) are shown for comparison (black dashed curve).

464 For comparison, equatorward jet shifts tend to occur less frequently in reanalysis (shown in black
465 in Fig. 5a) compared to model simulations with a free stratosphere, with a maximum frequency of
466 28 days within a 45-day period. A similar frequency is found for poleward jet shifts, with positive
467 zonal wind anomalies occurring in most cases for 27 days within a 45-day period, although a
468 relatively high frequency of positive anomalies is also found between 35 to 45 days. In fact, the
469 distribution of poleward shifts in the reanalysis resembles that of the free stratosphere run.

470 Thus, we show that equatorward jet shifts in the North Atlantic tend to become more frequent
471 within a period of 45 days in a model simulation with a free stratosphere as compared to the nudged
472 stratosphere simulation (Fig. 5), suggesting that the stratosphere, and SSW events in particular,
473 contribute to the occurrence of equatorward jet anomalies in North Atlantic. Equatorward jet shifts
474 in the model tend to be more frequent than in reanalysis, as indicated by the comparison with the
475 fraction of days with equatorward jet shifts in reanalysis, while poleward jet shifts on the other
476 hand have a similar frequency in both the model and the reanalysis. The enhanced frequency

of equatorward jet shifts in a simulation with stratospheric variability, compared to a simulation without stratospheric variability, is consistent with the Atlantic jet variability after SSW events as found in previous studies (Domeisen 2019, Fig1).

1) Role of the Northeastern Pacific for Atlantic jet shifts

The results shown in the previous section indicate that the stratosphere has an impact on the frequency of zonal wind shifts in the North Atlantic. Here we look specifically at the role of the northeastern Pacific driver and how it affects this behavior in the absence of stratospheric variability. As in the previous section, we compare the free stratosphere model simulation to the nudged stratosphere run, where the stratospheric zonal mean flow is nudged to climatology and hence the stratosphere does not contribute to Atlantic zonal wind anomalies.

Since SSW events do not occur in the nudged run, we can no longer compare the response to SSWs between the nudged and free stratosphere runs. Instead, we use a definition for "jet shift events" that can be applied in both the free and nudged simulations. According to our definition, an equatorward (poleward) jet shift event is detected if for a 45-day period (i) the North Atlantic zonal wind anomaly index (U'300) averaged over this 45-day period is negative (positive), and (ii) the fraction of days of the negative (positive) phase within this 45-day period is greater than 50%. This criterion is evaluated for each 45-day period in NDJFM, and an event can be identified immediately after a previous event. A similar definition has been used in Domeisen (2019) for the detection of NAO persistence events after SSWs. We detect all equatorward and poleward jet shift events in the free and nudged stratosphere runs. Anomalies are computed with respect to the daily climatology of the respective simulation. The same definition is applied in reanalysis, where jet shift events are defined during NDJFM for all the years between 1979 to 2019.

Consistent with the relationship obtained for the free stratosphere model run and the reanalysis (Fig. 3b), North Atlantic zonal wind anomalies during equatorward and poleward jet shift events in the nudged run are positively correlated with Pacific anomalies during the event (day 1 to 45) (Fig. 6a,c). For comparison, in the free stratosphere run, 33% of the explained variance for equatorward jet shift events can be attributed to the Pacific driver (Fig. 6a), which is more than three times the variance than can be explained by the Pacific driver in the nudged simulation (R^2=0.10, Fig. 6c), suggesting that without the stratospheric variability, the Pacific shows a limited impact

on the North Atlantic. In the reanalysis, a weaker correlation is found for equatorward jet shift events detected during NDJFM (Fig. 6e) (R^2=0.05, p>0.1) compared to the same type of events in the free stratosphere run (Fig. 6a) (R^2=0.33).

These results show that the Pacific circulation tends to have a stronger influence on the North Atlantic jet in the simulation with a free-evolving stratosphere (FREE) compared to the nudged-stratosphere (NUDGED) simulation, suggesting that without a stratospheric influence the Pacific-Atlantic correlation is weakened. This potentially highlights the role of the stratospheric pathway in linking northeastern Pacific variability with the North Atlantic. Thus, by excluding the stratospheric influence on both the North Atlantic and the northeastern Pacific, nudging the stratosphere allows us to isolate the direct impact of the Pacific on the downward impact in the Atlantic sector. According to this classification, Pacific contribution can explain up to 10% of the variance of North Atlantic conditions when there is no stratospheric variability.

2) The role of Atlantic internal variability

Another factor that may influence the outcome of the downward impact following SSW events is the existing tropospheric conditions in the Atlantic region. To examine whether the local Atlantic internal variability plays a role in the downward response, a comparison between the free stratosphere and nudged stratosphere runs is performed (Fig. 6). We examine both equatorward (blue line) and poleward (red) jet shift events.

We find that the relationship between zonal wind anomalies (ATL U'300) at the time of the onset of the event (days -2 to 2) and the anomalies during the event (days 1 to 45) is generally positive, both in the free-evolving (FREE) and the nudged stratosphere (NUDGED) runs (Fig. 6b and Fig. 6d, respectively), with stronger negative anomalies at the time of the event onset linked, on average, to a more negative impact (i.e., an equatorward jet shift).

In the free stratosphere run, a larger part of the variance of zonal wind anomalies during equatorward jet shift events can be explained by the circulation at the time of the event onset in that region (R^2=0.16, Fig. 6b), compared to a lower correlation in the nudged stratosphere run (R^2=0.11, Fig. 6d). A similar positive relation is found in the reanalysis (Fig. 6f), with nearly the same correlations as in the free stratosphere run (R^2=0.17 in FREE versus R^2=0.16 in the reanalysis).

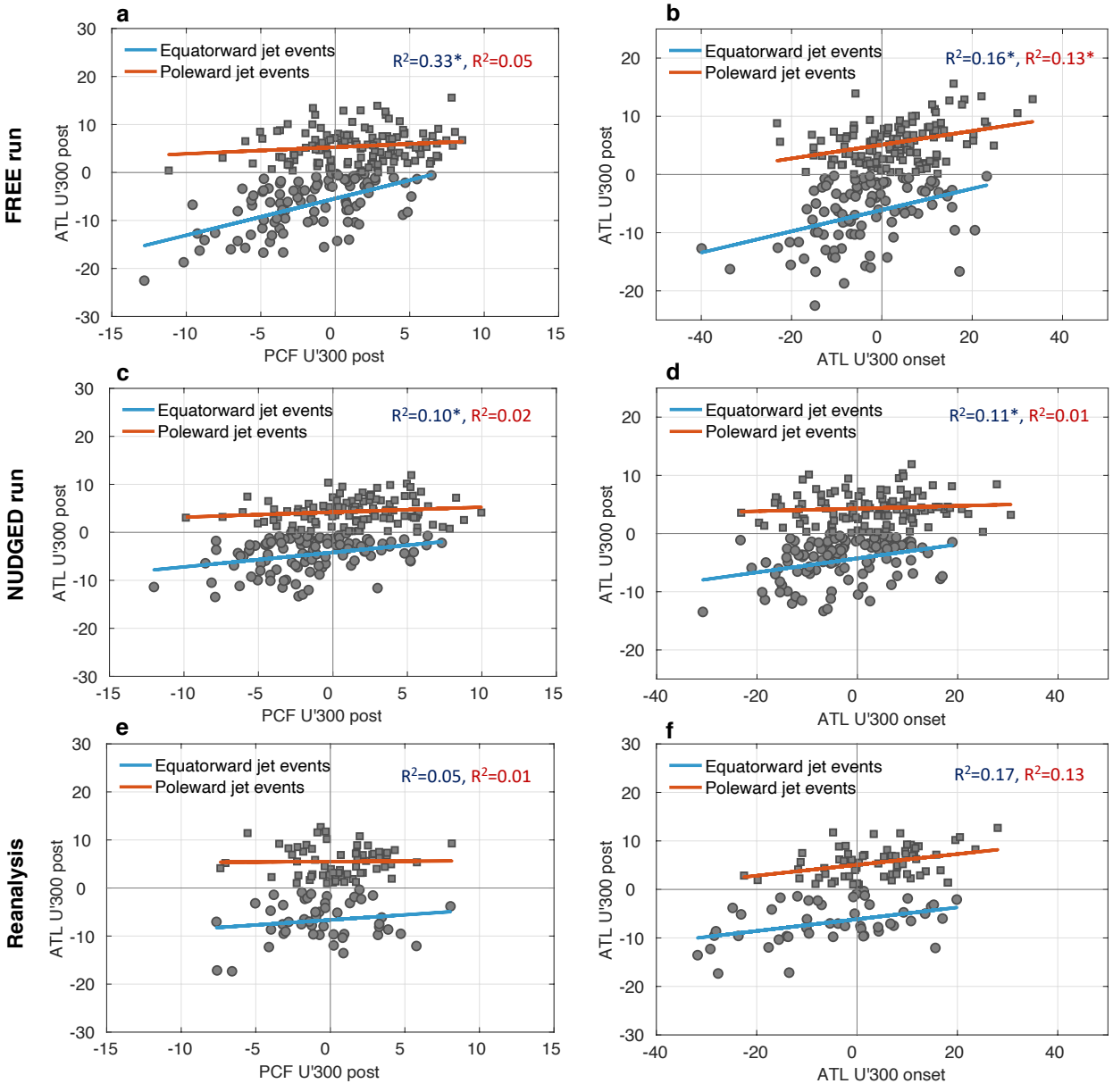

509 FIG. 6. (a,c,e) The relation between Atlantic zonal wind anomalies (ATL U'300), averaged between day 1 to 45
510 of jet shift events, and Pacific anomalies (PCF U'300) averaged over the same period in (a) the free stratosphere
511 run, (c) the nudged stratosphere run, and (e) ERA-Interim reanalysis. (b,d,f) Same as (a,c,e) but for the relation
512 with Atlantic zonal wind anomalies at the time of event onset (between day -2 to 2). Markers correspond to
513 averaged equatorward (circles) and poleward (squares) zonal wind anomalies in the Atlantic. R^2 values are
514 shown in each panel (all statistically significant correlations are marked by an asterisk, with p-values < 0.05).

This difference between equatorward jet events in nudged and free stratosphere runs suggests that stratospheric influence strengthens the persistence of these events (as indicated by the correlation between Atlantic zonal wind anomalies during a jet shift event and the same index at the time of the initial response). Local conditions in the North Atlantic play an equally important role for equatorward and poleward events in the free stratosphere model run and in the reanalysis.

4. Summary and discussion

This study investigates the tropospheric circulation response following SSW events and its connection with potential driving factors that affect the downward impact in the North Atlantic. For this purpose, we analyze the changes in North Atlantic zonal wind anomalies after SSW events in a intermediate-complexity GCM and in ERA-Interim reanalysis. We show that the variability of the downward response after SSW events is dependent at 30-day timescales) on both tropospheric and stratosphere influences. We identify two main factors that play a role in the downward impact in the North Atlantic during SSW events: The strength of the atmospheric circulation in the lower stratosphere, as measured by the polar cap geopotential height anomaly, and tropospheric zonal wind over the northeastern Pacific - North American region. Local Atlantic conditions at the time of SSW onset are also found to contribute to the sign of the downward response, particularly in the model.

Overall, the model realistically captures the ratio of equatorward-shifted to poleward-shifted tropospheric jet responses to SSWs; about two thirds of SSW events are dominated by the canonical equatorward Atlantic jet response, consistent with observations (Karpechko et al. 2017; Domeisen 2019; Afargan-Gerstman and Domeisen 2020). The large number of SSW events in the model (91 SSWs, compared to 26 SSWs in the reanalysis data from 1979–2019) allows us to explore their associated downward impact using a larger sample size than in the observational record in a simplified setting.

We find that in the North Atlantic, an equatorward jet shift (i.e., a canonical downward response) during days 1 to 30 after SSW events is strongly linked to positive geopotential height anomalies in the lower stratosphere (Fig. 3a). Such positive lower stratospheric anomalies are found following about 85% of SSW events both in the reanalysis and the model (Fig. 2a,c). These results also support previous studies, confirming the observation that the surface response to stratospheric forcing is

dependent on the persistence of lower stratospheric circulation anomalies (Black and McDaniel 2004; Hitchcock et al. 2013a; Maycock and Hitchcock 2015), as well as on their strength (e.g., Karpechko et al. 2017; Runde et al. 2016). More recently, it has been shown that the magnitude of the lower stratospheric warming is linearly related to the tropospheric response to SSW events in an idealized model study (White et al. 2020), and that strong SSWs are more likely to have a downward impact than weak SSWs in multimodel ensemble forecasts (Rao et al. 2020).

Another driver for the downward response is the negative zonal wind anomaly in the Northeast Pacific - North American region (Fig. 3b). These anomalies are found to be as important as the anomalies in the lower stratosphere after SSW events for an equatorward Atlantic jet response. In contrast, SSWs that are followed by a poleward jet response tend to be less affected by a single factor, suggesting a link to other potential factors, such as local Atlantic conditions at the time of the initial response or internal atmospheric variability. These results are consistent with previous studies showing that the tropospheric impacts of stratospheric extreme events depend, in addition to pre-existing anomalies in the lower stratosphere, also on the tropospheric conditions at the time of the downward impact (e.g., Black and McDaniel 2004; Chan and Plumb 2009; Domeisen et al. 2020a).

The relationship between the Atlantic jet response and these contributing factors is found to be stronger in the model compared to reanalysis (for the Pacific driver, this is also present in Fig. 2h). However, in this respect the similar ratio of SSW events that exhibit the equatorward-shifted downward impact relative to the poleward-shifted response in the model and reanalysis suggests that both the stratospheric and the Pacific influences may maintain their relative importance in the model despite exhibiting stronger individual correlations.

Analysis of the three drivers suggests that the lower stratosphere appears to play a more significant role for the downward impact, though tropospheric dynamics may contribute to the response. To isolate the tropospheric from the stratospheric influence, we use model runs for which the stratospheric zonal mean winds are nudged towards the model zonal mean climatology. In the absence of a stratospheric influence on the troposphere, the variability of the North Atlantic circulation is determined by tropospheric variability, i.e., an upstream influence from the northeastern Pacific as well as internal Atlantic variability. On average, the tropospheric influence is found to be weaker in the model when stratospheric variability is suppressed (Fig. 6c,d), compared to the free

stratosphere runs (Fig. 6a,b). This relationship, between the tropospheric drivers and the Atlantic jet response, is found to be more robust in the model compared to reanalysis for the northeastern Pacific driver, and similar to reanalysis for internal Atlantic variability.

Furthermore, we find that stratosphere strengthens the persistence of the tropospheric jet in the North Atlantic during periods of equatorward jet shifts. Local (i.e., indicated by the local conditions in the North Atlantic at the time of the onset of the jet shift event) precursors play a more important role for equatorward jet shifts than for poleward jet shifts. This difference implies that equatorward jet shift events seem to be more strongly influenced by external factors than the poleward events.

It is important to note that the various drivers investigated in this study are not independent of each other. However, while the effects of these drivers cannot be separated in reanalysis, the simplified model and particularly the nudged stratosphere experiment provide the opportunity to investigate the respective roles of the troposphere and the stratosphere. More specifically, while the stratosphere is acting to regulate the downstream impact (i.e., as indicated by the correlation with the lower stratospheric geopotential height anomalies), it could also be that the stratosphere directly forces the anomaly in the northeastern Pacific, which in turn leads to a downstream influence on the North Atlantic. In this context, analysis of the nudged stratosphere simulations suggests that the stratosphere strengthens the relation between tropospheric drivers in the model, implying that these drivers may not be independent of stratospheric influence. In addition, the large number of events in the model contributes to the statistical significance of the results.

The analysis presented in this study provides a clear picture of tropospheric jet changes in the midlatitude North Atlantic following SSW events. The tropospheric zonal wind response to SSWs is associated with a latitudinal shift of the jet that extends all the way to the surface (Fig. S1), and also affects the persistence of the atmospheric circulation. An increase in persistence of equatorward jet shifts (i.e., NAO-) after SSW events can lead to an enhanced risk of flooding over southern Europe due to the associated shift in the storm track activity (e.g., Rao et al. 2020; Domeisen and Butler 2020). These findings may shed light on the contribution of the stratosphere to the type of the downward impact of SSW events, and help to improve the predictability of the North Atlantic tropospheric jet response. Specifically, by identifying the key drivers for the downward impact in the simplified model, the role of the stratosphere, as well as other remote drivers, in sub-seasonal to seasonal prediction systems can be assessed and improved. Furthermore, combining

our analysis with a tracking algorithm (e.g., Hall et al. 2020) or techniques for identification of causal relationships could provide further insights on the causality of the downward impact in future research.

Acknowledgments. Support from the Swiss National Science Foundation through project PP00P2_170523 to H.A.-G. and both PP00P2_170523 and PP00P2_198896 to D.D. is gratefully acknowledged. This project has received funding from the European Research Council (ERC) under the European Union's Horizon 2020 research and innovation programme (grant agreement No. 847456), and from the European Union's Horizon 2020 research and innovation programme under the Marie Sklodowska-Curie (MSC) (grant agreement No. 891514). The authors would like to thank three anonymous reviewers for their comments that helped to improve the manuscript. H.A.-G. would also like to thank Maria Pyrina for useful discussions.

Data availability statement. The Isca modeling framework can be downloaded from the GitHub repository (https://github.com/ExeClim/Isca, last access: August 2021) (Vallis et al. 2018). The ERA-Interim reanalysis has been obtained from the ECMWF server (https://apps.ecmwf.int/datasets/data/interim-full-daily/levtype=sfc/, last access: August 2021) (Dee et al. 2011).

References

Afargan-Gerstman, H., and D. I. V. Domeisen, 2020: Pacific modulation of the North Atlantic storm track response to sudden stratospheric warming events. *Geophysical Research Letters*, **47**, e2019GL085 007, https://doi.org/10.1029/2019GL085007.

Afargan-Gerstman, H., I. Polkova, L. Papritz, P. Ruggieri, M. P. King, P. J. Athanasiadis, J. Baehr, and D. I. Domeisen, 2020: Stratospheric influence on north atlantic marine cold air outbreaks following sudden stratospheric warming events. *Weather and Climate Dynamics*, **1 (2)**, 541–553.

Baldwin, M. P., and T. J. Dunkerton, 2001: Stratospheric harbingers of anomalous weather regimes. *Science*, **294 (5542)**, 581–584.

Baldwin, M. P., and D. W. Thompson, 2009: A critical comparison of stratosphere–troposphere coupling indices. *Quarterly Journal of the Royal Meteorological Society*, **135 (644)**, 1661–1672.

Baldwin, M. P., and Coauthors, 2021: Sudden Stratospheric Warmings. *Reviews of Geophysics*, **59 (1)**.

Benedict, J. J., S. Lee, and S. B. Feldstein, 2004: Synoptic view of the north atlantic oscillation. *Journal of the atmospheric sciences*, **61 (2)**, 121–144.

Black, R. X., and B. A. McDaniel, 2004: Diagnostic case studies of the northern annular mode. *Journal of climate*, **17 (20)**, 3990–4004.

Butler, A. H., D. J. Seidel, S. C. Hardiman, N. Butchart, T. Birner, and A. Match, 2015: Defining sudden stratospheric warmings. *Bulletin of the American Meteorological Society*, **96 (11)**, 1913–1928.

Butler, A. H., J. P. Sjoberg, D. J. Seidel, and K. H. Rosenlof, 2017: A sudden stratospheric warming compendium. *Earth System Science Data*, **9 (1)**.

Chan, C. J., and R. A. Plumb, 2009: The response to stratospheric forcing and its dependence on the state of the troposphere. *Journal of the Atmospheric Sciences*, **66 (7)**, 2107–2115.

Charlton, A. J., and L. M. Polvani, 2007: A new look at stratospheric sudden warmings. part i: Climatology and modeling benchmarks. *Journal of Climate*, **20 (3)**, 449–469.

Charlton-Perez, A. J., L. Ferranti, and R. W. Lee, 2018: The influence of the stratospheric state on North Atlantic weather regimes. *Quarterly Journal of the Royal Meteorological Society*, **144 (713)**, 1140–1151.

Dee, D. P., and Coauthors, 2011: The ERA-Interim reanalysis: Configuration and performance of the data assimilation system. *Quarterly Journal of the royal meteorological society*, **137 (656)**, 553–597.

Domeisen, D. I. V., 2019: Estimating the frequency of sudden stratospheric warming events from surface observations of the North Atlantic oscillation. *Journal of Geophysical Research: Atmospheres*, **124 (6)**, 3180–3194.

Domeisen, D. I. V., and A. H. Butler, 2020: Stratospheric drivers of extreme events at the earth's surface. *Communications Earth & Environment*, **1 (1)**, 1–8.

683 Domeisen, D. I. V., A. H. Butler, K. Fröhlich, M. Bittner, W. A. Müller, and J. Baehr, 2015:
684 Seasonal predictability over Europe arising from El Niño and stratospheric variability in the
685 MPI-ESM seasonal prediction system. *Journal of Climate*, **28 (1)**, 256–271.

686 Domeisen, D. I. V., C. M. Grams, and L. Papritz, 2020a: The role of North Atlantic-European
687 weather regimes in the surface impact of sudden stratospheric warming events. *Weather and*
688 *Climate Dynamics*, **1**, 373–388, https://doi.org/10.5194/wcd-1-373-2020.

689 Domeisen, D. I. V., L. Sun, and G. Chen, 2013: The role of synoptic eddies in the tropospheric
690 response to stratospheric variability. *Geophysical Research Letters*, **40 (18)**, 4933–4937.

691 Domeisen, D. I. V., and Coauthors, 2020b: The Role of the Stratosphere in Subseasonal to
692 Seasonal Prediction: 2. Predictability Arising From Stratosphere-Troposphere Coupling. *Journal*
693 *of Geophysical Research-Atmospheres*, **125 (2)**, 1–20.

694 Drouard, M., G. Rivière, and P. Arbogast, 2015: The link between the North Pacific climate
695 variability and the North Atlantic Oscillation via downstream propagation of synoptic waves. *J.*
696 *Climate*, **28 (10)**, 3957–3976.

697 Franzke, C., S. Lee, and S. B. Feldstein, 2004: Is the North Atlantic Oscillation a breaking wave?
698 *Journal of the Atmospheric Sciences*, **61 (2)**, 145–160.

699 Garfinkel, C. I., D. W. Waugh, and E. P. Gerber, 2013: The effect of tropospheric jet latitude on
700 coupling between the stratospheric polar vortex and the troposphere. *Journal of Climate*, **26 (6)**,
701 2077–2095.

702 Gerber, E. P., and L. M. Polvani, 2009: Stratosphere–troposphere coupling in a relatively simple
703 agcm: The importance of stratospheric variability. *Journal of Climate*, **22 (8)**, 1920–1933.

704 Hall, R. J., D. M. Mitchell, W. J. Seviour, and C. J. Wright, 2020: Tracking the stratosphere-
705 to-surface impact of sudden stratospheric warmings. *Journal of Geophysical Research: Atmo-*
706 *spheres*, e2020JD033881.

707 Hitchcock, P., T. G. Shepherd, and G. L. Manney, 2013a: Statistical characterization of Arctic
708 polar-night jet oscillation events. *Journal of Climate*, **26 (6)**, 2096–2116.

Hitchcock, P., T. G. Shepherd, M. Taguchi, S. Yoden, and S. Noguchi, 2013b: Lower-stratospheric radiative damping and polar-night jet oscillation events. *Journal of the Atmospheric Sciences*, **70 (5)**, 1391–1408.

Hitchcock, P., and I. R. Simpson, 2016: Quantifying eddy feedbacks and forcings in the tropospheric response to stratospheric sudden warmings. *Journal of the Atmospheric Sciences*, **73 (9)**, 3641–3657.

Huang, B., and Coauthors, 2015: Extended reconstructed sea surface temperature version 4 (ERSST. v4). Part I: Upgrades and intercomparisons. *Journal of climate*, **28 (3)**, 911–930.

Jiménez-Esteve, B., and D. I. V. Domeisen, 2018: The tropospheric pathway of the ENSO–North Atlantic teleconnection. *Journal of Climate*, **31 (11)**, 4563–4584.

Jiménez-Esteve, B., and D. I. V. Domeisen, 2019: Nonlinearity in the North Pacific atmospheric response to a linear ENSO forcing. *Geophysical Research Letters*, **46 (4)**, 2271–2281.

Jiménez Esteve, B., and D. I. V. Domeisen, 2020: Nonlinearity in the tropospheric pathway of ENSO to the North Atlantic. *Weather and Climate Dynamics*, **1 (1)**, 225–245.

Jucker, M., 2016: Are sudden stratospheric warmings generic? Insights from an idealized GCM. *Journal of the Atmospheric Sciences*, **73 (12)**, 5061–5080.

Jucker, M., and E. Gerber, 2017: Untangling the annual cycle of the tropical tropopause layer with an idealized moist model. *Journal of Climate*, **30 (18)**, 7339–7358.

Karpechko, A. Y., A. Charlton-Perez, M. Balmaseda, N. Tyrrell, and F. Vitart, 2018: Predicting sudden stratospheric warming 2018 and its climate impacts with a multimodel ensemble. *Geophysical Research Letters*, **45 (24)**, 13–538.

Karpechko, A. Y., P. Hitchcock, D. H. Peters, and A. Schneidereit, 2017: Predictability of downward propagation of major sudden stratospheric warmings. *Quarterly Journal of the Royal Meteorological Society*, **143 (704)**, 1459–1470.

Kidston, J., A. A. Scaife, S. C. Hardiman, D. M. Mitchell, N. Butchart, M. P. Baldwin, and L. J. Gray, 2015: Stratospheric influence on tropospheric jet streams, storm tracks and surface weather. *Nature Geoscience*, **8 (6)**, 433.

King, A. D., A. H. Butler, M. Jucker, N. O. Earl, and I. Rudeva, 2019: Observed relationships between Sudden Stratospheric Warmings and European climate extremes. *Journal of Geophysical Research: Atmospheres*, **124 (24)**, 13 943–13 961.

Kodera, K., H. Mukougawa, P. Maury, M. Ueda, and C. Claud, 2016: Absorbing and reflecting sudden stratospheric warming events and their relationship with tropospheric circulation. *Journal of Geophysical Research: Atmospheres*, **121 (1)**, 80–94.

Kolstad, E. W., T. Breiteig, and A. A. Scaife, 2010: The association between stratospheric weak polar vortex events and cold air outbreaks in the Northern Hemisphere. *Quarterly Journal of the Royal Meteorological Society*, **136 (649)**, 886–893.

Lehtonen, I., and A. Y. Karpechko, 2016: Observed and modeled tropospheric cold anomalies associated with sudden stratospheric warmings. *Journal of Geophysical Research: Atmospheres*, **121 (4)**, 1591–1610.

Lu, Q., J. Rao, Z. Liang, D. Guo, J. Luo, S. Liu, C. Wang, and T. Wang, 2021: The sudden stratospheric warming in january 2021. *Environmental Research Letters*, **16 (8)**, 084 029.

Martineau, P., and S.-W. Son, 2013: Planetary-scale wave activity as a source of varying tropospheric response to stratospheric sudden warming events: A case study. *Journal of Geophysical Research: Atmospheres*, **118 (19)**, 10–994.

Maycock, A. C., and P. Hitchcock, 2015: Do split and displacement sudden stratospheric warmings have different annular mode signatures? *Geophysical Research Letters*, **42 (24)**, 10–943.

Mitchell, D. M., L. J. Gray, J. Anstey, M. P. Baldwin, and A. J. Charlton-Perez, 2013: The influence of stratospheric vortex displacements and splits on surface climate. *Journal of Climate*, **26 (8)**, 2668–2682.

Mlawer, E. J., S. J. Taubman, P. D. Brown, M. J. Iacono, and S. A. Clough, 1997: Radiative transfer for inhomogeneous atmospheres: RRTM, a validated correlated-k model for the longwave. *Journal of Geophysical Research: Atmospheres*, **102 (D14)**, 16 663–16 682.

Rao, J., C. I. Garfinkel, and I. P. White, 2020: Predicting the downward and surface influence of the february 2018 and january 2019 sudden stratospheric warming events in subseasonal to seasonal (s2s) models. *Journal of Geophysical Research: Atmospheres*, **125 (2)**, e2019JD031 919.

Rao, J., R. Ren, H. Chen, Y. Yu, and Y. Zhou, 2018: The stratospheric sudden warming event in february 2018 and its prediction by a climate system model. *Journal of Geophysical Research: Atmospheres*, **123 (23)**, 13–332.

Rivière, G., P. Arbogast, and A. Joly, 2015: Eddy kinetic energy redistribution within idealized extratropical cyclones using a two-layer quasi-geostrophic model. *Q. J. R. Meteorol. Soc.*, **141 (686)**, 207–223.

Runde, T., M. Dameris, H. Garny, and D. Kinnison, 2016: Classification of stratospheric extreme events according to their downward propagation to the troposphere. *Geophysical Research Letters*, **43 (12)**, 6665–6672.

Scaife, A., and Coauthors, 2016: Seasonal winter forecasts and the stratosphere. *Atmospheric Science Letters*, **17 (1)**, 51–56.

Scaife, A. A., J. R. Knight, G. K. Vallis, and C. K. Folland, 2005: A stratospheric influence on the winter NAO and North Atlantic surface climate. *Geophysical Research Letters*, **32 (18)**.

Scherhag, R., 1952: Die explosionartigen stratospharenwarmungen des spatwinters 1951-1952. *Ber. Deut. Wetterd.*, **6**, 51–63.

Seviour, W. J., L. J. Gray, and D. M. Mitchell, 2016: Stratospheric polar vortex splits and displacements in the high-top cmip5 climate models. *Journal of Geophysical Research: Atmospheres*, **121 (4)**, 1400–1413.

Seviour, W. J., D. M. Mitchell, and L. J. Gray, 2013: A practical method to identify displaced and split stratospheric polar vortex events. *Geophysical Research Letters*, **40 (19)**, 5268–5273.

Sigmond, M., J. Scinocca, V. Kharin, and T. Shepherd, 2013: Enhanced seasonal forecast skill following stratospheric sudden warmings. *Nature Geoscience*, **6 (2)**, 98.

Smith, K. L., and R. K. Scott, 2016: The role of planetary waves in the tropospheric jet response to stratospheric cooling. *Geophysical Research Letters*, **43 (6)**, 2904–2911.

Song, Y., and W. A. Robinson, 2004: Dynamical mechanisms for stratospheric influences on the troposphere. *Journal of the atmospheric sciences*, **61 (14)**, 1711–1725.

Thomson, S. I., and G. K. Vallis, 2018: Atmospheric response to sst anomalies. part i: Background-state dependence, teleconnections, and local effects in winter. *Journal of the Atmospheric Sciences*, **75 (12)**, 4107–4124.

Vallis, G. K., and Coauthors, 2018: Isca, v1.0: a framework for the global modelling of the atmospheres of Earth and other planets at varying levels of complexity. *Geoscientific Model Development*, **11**, 843–859.

White, I., C. I. Garfinkel, E. P. Gerber, M. Jucker, V. Aquila, and L. D. Oman, 2019: The downward influence of sudden stratospheric warmings: association with tropospheric precursors. *Journal of Climate*, **32 (1)**, 85–108.

White, I. P., C. I. Garfinkel, E. P. Gerber, M. Jucker, P. Hitchcock, and J. Rao, 2020: The Generic Nature of the Tropospheric Response to Sudden Stratospheric Warmings. *Journal of Climate*, **33 (13)**, 5589–5610.

Woollings, T., A. Hannachi, and B. Hoskins, 2010: Variability of the North Atlantic eddy-driven jet stream. *Q. J. R. Meteorol. Soc.*, **136 (649)**, 856–868.

Wright, C. J., R. J. Hall, T. P. Banyard, N. P. Hindley, I. Krisch, D. M. Mitchell, and W. J. Seviour, 2021: Dynamical and surface impacts of the January 2021 sudden stratospheric warming in novel Aeolus wind observations, MLS and ERA5. *Weather and Climate Dynamics*, **2 (4)**, 1283–1301.